



Rapid degradation of biomedical magnesium induced by zinc ion implantation

Guosong Wu, Li Gong, Kai Feng, Shuilin Wu, Ying Zhao, Paul K. Chu*

Department of Physics and Materials Science, City University of Hong Kong, Tat Chee Avenue, Kowloon, Hong Kong

ARTICLE INFO

Article history:

Received 30 October 2010

Accepted 24 November 2010

Available online xxx

Keywords:

Magnesium
Biomaterials
Ion implantation
Degradation
Surface

ABSTRACT

The degradation rate is important to biodegradable magnesium materials. In this study, Zn is implanted using a cathodic arc source into pure magnesium at an accelerating voltage of 35 kV. The nominal ion implant fluence is 2.5×10^{17} ions cm^{-2} . After Zn implantation, the degradation rate in simulated body fluids is increased significantly. It is postulated that because Zn exists in the metallic state in the implanted layer, the galvanic effect between the Zn rich surface region and magnesium matrix induces the observed accelerated degradation.

© 2010 Elsevier B.V. All rights reserved.

1. Introduction

Commercial applications of magnesium and magnesium alloys have been hampered by their intrinsic properties such as low mechanical strength and poor corrosion resistance compared to other metals such as titanium and stainless steels [1]. However, the materials degrade naturally in the physiological environment and there has been increasing interest in developing biodegradable Mg-based materials for clinical applications such as orthopedics and dentistry. In fact, in addition to its natural degradability, magnesium has another favorable biomedical property in that its Young's modulus of about 40 GPa is similar to that of human bone [2–4]. Clinically, the healing period after implantation of the surgical instruments into the human body depends on the conditions of the affected tissue. Unfortunately for raw magnesium and its alloys, their biodegradation rate is not acceptable and attempts have been made to control the degradation rate to suit biomedical application [5,6]. Coatings are considered to be effective in lowering the degradation rate of magnesium materials in the physiological environment. For instance, Al_2O_3 coatings have been proposed to reduce the corrosion rate of biodegradable magnesium alloys [7]. However, because most ceramic coatings are chemically inert, this approach may compromise the eventual bio-integrability between the artificial materials and body tissues.

Some biodegradable polymers such as polyglycolide, polylactide and polycaprolactone not only possess good biocompatibility but also exhibit lower degradation rates than magnesium materials [8,9]. Hence, if magnesium substrates are coated with such polymeric films, surface degradation can be mitigated. For example, we deposited a degradable polymer coating made of polycaprolactone (PCL) and

dichloromethane (DCM) onto magnesium alloys and successfully retarded the degradation rate both *in vitro* and *in vivo* [10]. On the heels of our success, we propose a new polymer/magnesium structure model as shown in Fig. 1 that is potentially applicable to blood vessels, urethra, biliary tracts, intestinal canals and esophagus. In this technique, the magnesium substrate is protected by the degradable polymer coating in the physiological environment and effectively supports the affected tissues during healing. After the healing period, the magnesium substrate loses the protective layer and intrinsic degradation occurs. Obviously, it is still necessary to develop a surface treatment protocol that allows the suitable degradation rate in this step without causing psychological harm and significant impairment to the human body.

Besides coating techniques, ion implantation can be utilized to control the degradation rate of magnesium and its alloys and both decelerated and accelerated degradation effects have been reported [11,12]. It should be noted that because of the limited ion energy, the implanted layer is usually not very thick and so may not resist corrosion as effectively as thicker ceramic coatings. Zn is one of the vital elements and has been incorporated into biomedical materials such as Mg–Zn alloys [13,14]. In this study, we investigate the effects of Zn ion implantation on the biodegradation of pure magnesium in simulated physiological conditions.

2. Experimental details

As-cast magnesium plates (99.95% pure and $10 \times 10 \times 5 \text{ mm}^3$) were mechanically polished using up to $1 \mu\text{m}$ diamond paste, ultrasonically washed in pure ethanol, and dried prior to Zn ion implantation. An HEMII-80 ion implanter equipped with a zinc cathodic arc source manufactured by Plasma Technology Ltd. was used to conduct Zn ion implantation. The base pressure in the vacuum chamber was $1.8 \times 10^{-4} \text{ Pa}$ and the implantation time was 1 h. The

* Corresponding author. Tel.: +852 34427724; fax: +852 34420542.
E-mail address: paul.chu@cityu.edu.hk (P.K. Chu).

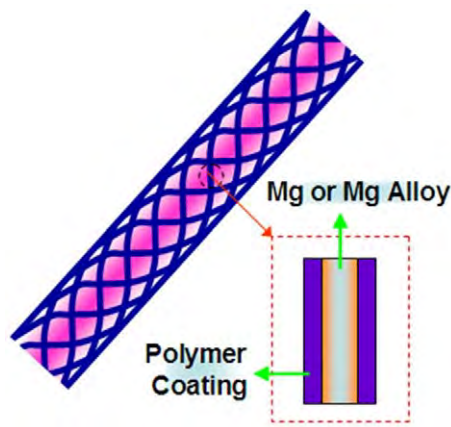


Fig. 1. Schematic diagram of a representative stent made of polymer-coated Mg materials.

zinc ions were accelerated by a voltage of about 35 kV and the nominal ion implant fluence was 2.5×10^{17} ions cm^{-2} . The average projected range determined by TRIM was about 47 nm.

X-ray photoelectron spectroscopy (XPS) with Al K_{α} irradiation was used to determine the chemical states and elemental depth profiles before and after ion implantation. The sputtering rate was estimated to be about 0.034 nm s^{-1} based on the rate calculated from a standard SiO_2 film sputtered under the same conditions. The binding energies were referenced to the C 1s line at 285.0 eV. Simulated body fluids (SBF) [11] were prepared to evaluate the biodegradation of the specimens. The electrochemical experiment was carried out on a

Zahner Zennium electrochemical workstation using the conventional three-electrode technique. The potential was referred to a saturated calomel electrode (SCE) and the counter electrode was a platinum sheet. The specimens with a surface area of $10 \times 10 \text{ mm}^2$ were exposed to the SBF solution and the test was carried out at 1 mV/s at 37°C . An immersion test was further performed to evaluate the degradation. The surface and cross-section of the specimens were observed after immersion in SBF for 18 h at 37°C . An MTS nano-indenter was utilized to evaluate the hardness and elastic modulus values of the specimens.

3. Results and discussion

Fig. 2 shows the XPS results of the pure and Zn implanted magnesium samples. It can be observed that a zinc rich layer is formed near the surface after ion implantation. Generally, the shift in the Zn LMM Auger peak is an indicator of chemical state changes. The peak near 992.1 eV corresponds to zinc in the metallic state whereas the peak near 988.5 eV is associated with zinc in the oxidized state [15]. Here, no evident shift is observed during sputtering, indicating that zinc in the implanted layer is in the metallic state. As the sputtering time increases, the oxygen content gradually decreases and the Mg 1s peak shifts from about 1304.5 eV to 1303.0 eV. It means that an oxide layer is formed on the surface when the sample is exposed to air. Because MgCO_3 , $\text{Mg}(\text{OH})_2$, and MgO are probably formed on the top surface when Mg and Mg alloys are exposed to air [16,17], there exists a slight difference in the O 1s peak between a sputtering time of 10 s and others.

Fig. 3(a) displays the polarization curves of the samples in SBF. The curve obtained from the implanted magnesium sample shifts to a higher

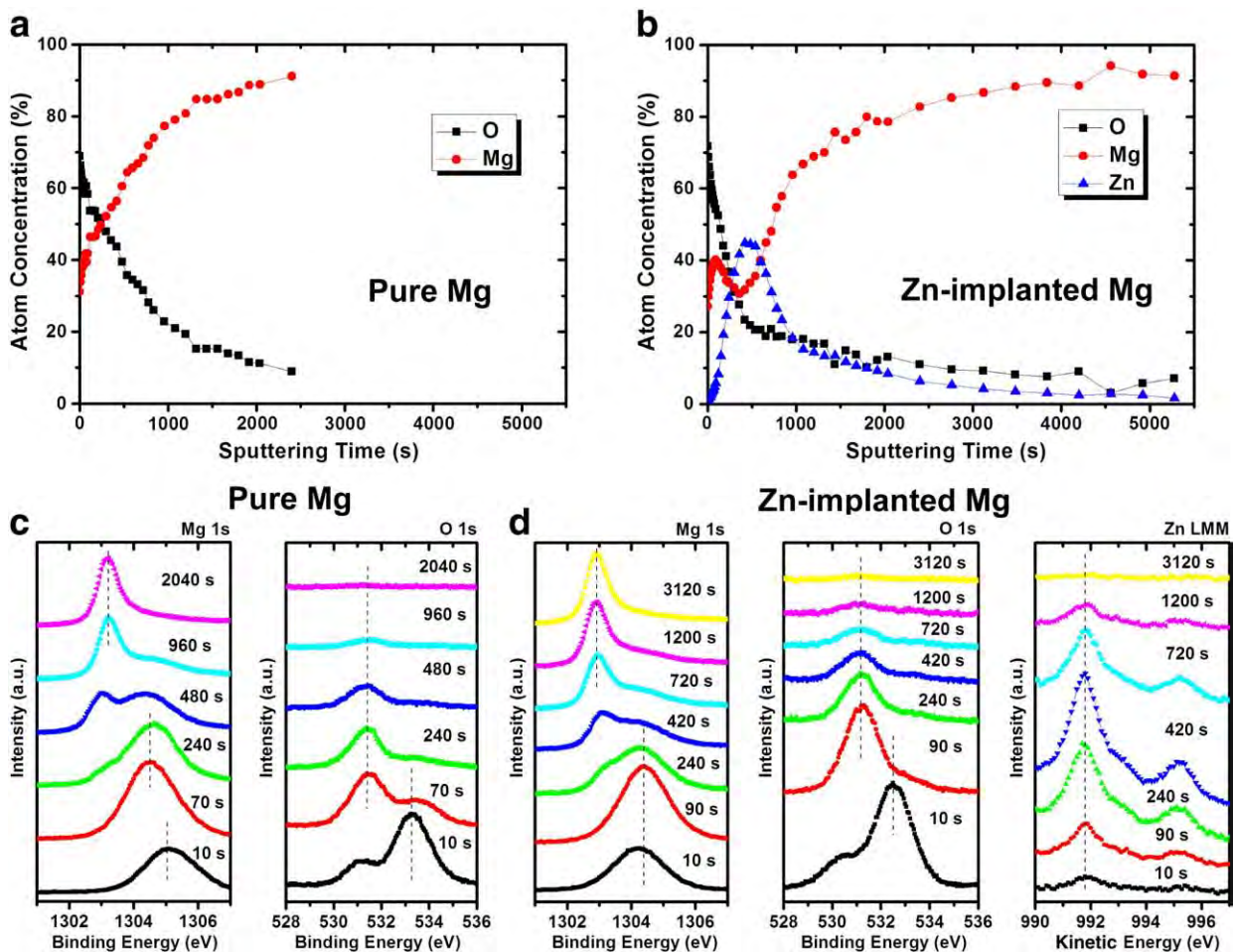


Fig. 2. XPS depth profiles of (a) pure magnesium and (b) Zn implanted magnesium. High-resolution XPS spectra of (c) pure magnesium and (d) Zn implanted magnesium.

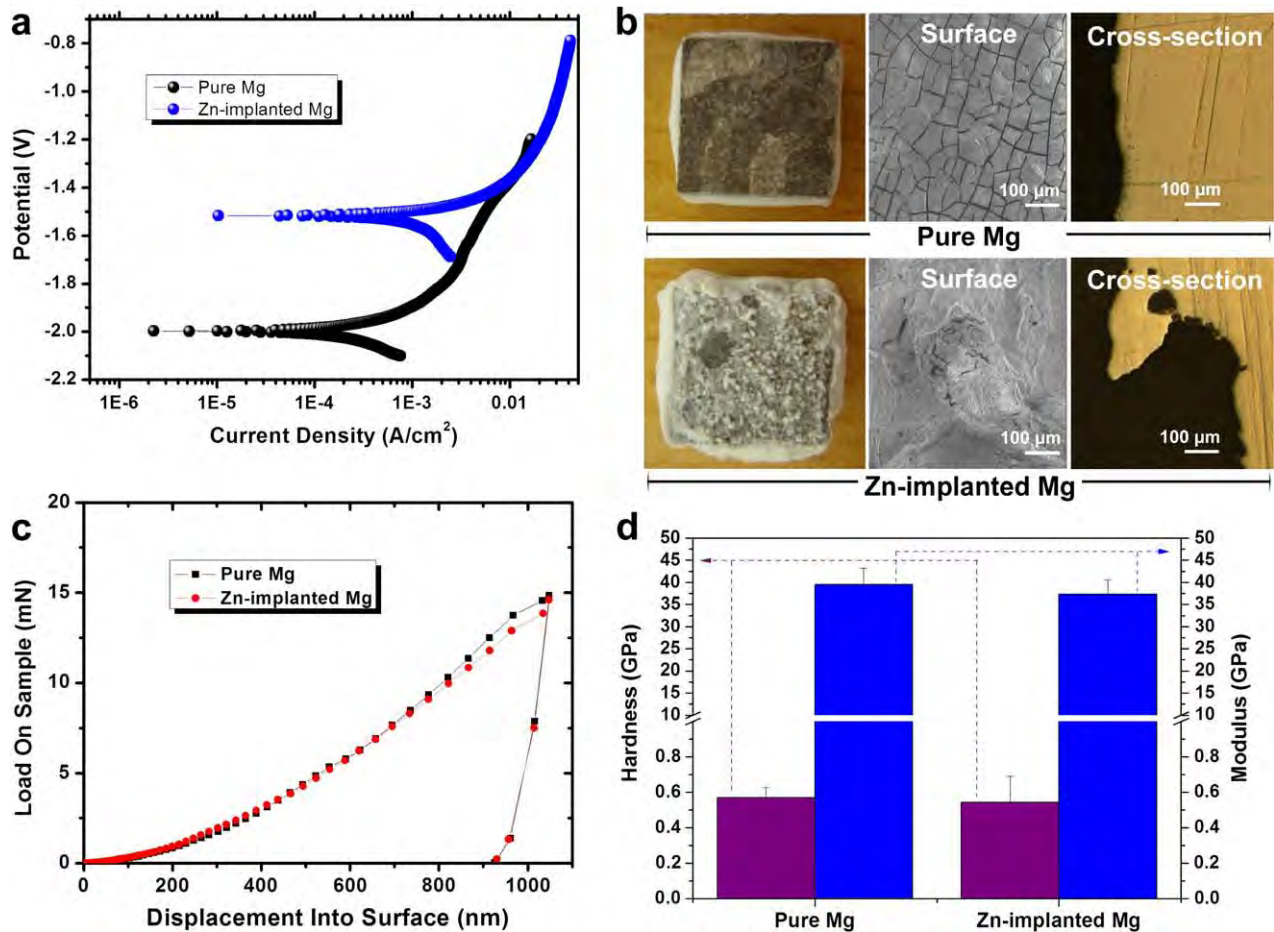


Fig. 3. (a) Polarization curves of pure magnesium and Zn implanted magnesium in SBF. (b) Surface and cross-section pictures of the samples after immersion in SBF for 18 h. (c) Load on sample as a function of displacement into surface. (d) Hardness and elastic modulus of pure magnesium and Zn implanted magnesium.

current density and higher potential. In this study, the corrosion potential and corrosion current density are derived directly from the region in the cathodic polarization curves by Tafel region extrapolation. The corrosion potential of the implanted sample increases from -1.998 V to -1.517 V and its corrosion current density increases from 1.738×10^{-4} A/cm² to 1.147×10^{-3} A/cm². The higher the corrosion current density, the lower is the corrosion resistance and therefore, the degradation rate of magnesium is evidently increased by ion implantation. Fig. 3(b) illustrates the results of the immersion test. After 18 h of immersion in SBF, white degradation products are observed on the surface of the implanted sample. Both the surface and cross-section pictures disclose that the Zn implanted sample suffers from more severe local corrosion than pure magnesium. According to the XPS analysis, a thin Zn rich layer where Zn exists in the metallic state is formed near the top surface after ion implantation and so galvanic corrosion is prone to happen between the Zn rich region and Mg matrix in SBF. Furthermore, as described in the literature [12,18], ion implantation introduces defects to the surface providing short cuts to accelerate galvanic corrosion. Fig. 3(c) shows the load–displacement curves and Fig. 3(d) presents the hardness and elastic modulus. No significant difference in the hardness and modulus can be observed between the pure magnesium and Zn implanted sample. In other words, in spite of the difference in the corrosion resistance, Zn ion implantation does not alter the surface mechanical properties of magnesium appreciably.

4. Conclusion

A thin Zn rich surface layer with Zn existing in the metallic state is formed by ion implantation. The degradation rate of pure magnesium

in simulated body fluids is increased after Zn ion implantation due to the galvanic effect. In spite of the change in the corrosion characteristics, Zn ion implantation does not affect the surface mechanical properties of magnesium.

Acknowledgement

This study was supported by the Hong Kong Research Grants Council (RGC) General Research Funds (GRF) No. CityU 112510.

References

- [1] Gray JE, Luan B. *J Alloys Compd* 2002;336:88–113.
- [2] Zberg B, Uggowitzer PJ, Löffler JF. *Nat Mater* 2009;8:887–91.
- [3] Zhang E, Xu L, Yang K. *Scr Mater* 2005;53:523–7.
- [4] Song Y, Shan D, Chen R, Zhang F, Han EH. *Mater Sci Eng C* 2009;29:1039–45.
- [5] Song GL. *Corros Sci* 2007;49:1696–701.
- [6] Hiromoto S, Yamamoto A. *Mater Sci Eng C* 2010;30:1085–93.
- [7] Xin Y, Liu C, Zhang W, Jiang J, Chu PK. *J Electrochem Soc* 2008;155(5):C178–82.
- [8] Hutmacher DW. *Biomaterials* 2000;21:2529–43.
- [9] Yoshimoto H, Shin YM, Terai H, Vacanti JP. *Biomaterials* 2003;24:2077–82.
- [10] Wong HM, Yeung WK, Chu PK, Luk DK, Cheung MC. *Biomaterials* 2010;31:2084–96.
- [11] Liu C, Xin Y, Tian Xi, Zhao J, Chu PK. *J Vac Sci Technol A* 2007;25(2):334–9.
- [12] Wu G, Zeng X, Yao S, Han H. *Mater Sci Forum* 2007;546–549:551–4.
- [13] Gu X, Zheng Y, Cheng Y, Zhong S, Xi T. *Biomaterials* 2009;30:484–98.
- [14] Gu X, Zheng Y, Zhong S, Xi T, Wang J, Wang W. *Biomaterials* 2010;31:1093–103.
- [15] Moulder JF, Stickle WF, Sobol PE, Bomben KD, Chastain J. *Handbook of X-ray Photoelectron Spectroscopy*. Minnesota: Perkin-Elmer Corporation, Physical Electronics Division; 1992.
- [16] Wu G, Dai W, Song L, Wang A. *Mater Lett* 2010;64:475–8.
- [17] Wu G, Zeng X, Yuan G. *Mater Lett* 2008;62:4325–7.
- [18] Wu G, Ding K, Zeng X, Wang X, Yao S. *Scr Mater* 2009;61:269–72.